



## Photoluminescence Properties of Green-Emitting ZnGa<sub>2</sub>S<sub>4</sub>:Eu<sup>2+</sup> Phosphor

Ruijin Yu,<sup>a,b</sup> Ruixin Luan,<sup>a</sup> Caifeng Wang,<sup>a</sup> Jingtao Chen,<sup>a</sup> Zhenxing Wang,<sup>a</sup> Byung Kee Moon,<sup>b</sup> and Jung Hyun Jeong<sup>b,\*</sup>

<sup>a</sup>College of Science, Northwest A&F University, Yangling, Shaanxi 712100, China

<sup>b</sup>Department of Physics, Pukyong National University, Busan 608-737, South Korea

Green-emitting ZnGa<sub>2</sub>S<sub>4</sub>:Eu<sup>2+</sup> phosphors have been synthesized by solid state reaction. Their luminescence properties have been investigated by photoluminescence excitation and emission spectra, concentration quenching, thermal quenching and photoluminescence decay. The critical dopant concentration is found to be 0.05 mol of Eu<sup>2+</sup> and the critical transfer distance of Eu<sup>2+</sup> is calculated as 17 Å. The thermal quenching result suggests that the phosphor does not have good thermal-quenching property. Its chromaticity coordinates are very close to those of SrGa<sub>2</sub>S<sub>4</sub>:Eu<sup>2+</sup>. Because of their broadband absorption in the region 350–520 nm, the ZnGa<sub>2</sub>S<sub>4</sub>:0.05Eu<sup>2+</sup> phosphor can be a good green phosphor candidate for creating white light in phosphor-converted white LEDs, when combined with RB phosphors and a UV LED.

© 2012 The Electrochemical Society. [DOI: 10.1149/2.099205jes] All rights reserved.

Manuscript submitted December 23, 2011; revised manuscript received February 13, 2012. Published March 7, 2012.

Luminescence properties of the ternary compounds M<sup>II</sup>M<sub>2</sub><sup>III</sup>(S,Se)<sub>4</sub> doped with various rare earth ions have been investigated during the past decades.<sup>1–6</sup> Nowadays, the compounds have been paid more attention to another potential application for phosphor converted light-emitting diodes (pc-LEDs) as solid-state lighting (SSL). CaGa<sub>2</sub>S<sub>4</sub>:Eu<sup>2+</sup>, Sr<sub>2</sub>Ga<sub>2</sub>S<sub>5</sub>:Eu<sup>2+</sup> greenish-yellow phosphors showed a higher luminescent efficiency (120, 110%, respectively) than commercial Y<sub>3</sub>Al<sub>5</sub>O<sub>12</sub>:Ce<sup>3+</sup> (YAG:Ce<sup>3+</sup>) phosphor and they also can be fabricated with blue-chips to produce white light.<sup>7,8</sup> SrGa<sub>2</sub>S<sub>4</sub>:Eu<sup>2+</sup> has a wide excitation band extending into the blue region, it is applicable as a green phosphor for white LEDs in which blue LEDs are used to excite the phosphor.<sup>9,10</sup> SrGa<sub>2</sub>S<sub>4</sub>:Sn,Re (Re = Ce, Gd) also has been studied as possible phosphors of white LEDs.<sup>11</sup> Yu et al. described the structural and luminescent properties of Ca<sub>1–x</sub>Sr<sub>x</sub>(Ga<sub>1–y</sub>Al<sub>y</sub>)<sub>2</sub>S<sub>4</sub>:Eu<sup>2+</sup> phosphors. Changing the values of *x* and *y*, the emission peak shifts almost linearly on the composition, which allows continuous tuning of the peak emission peak from 496 nm (SrAl<sub>2</sub>S<sub>4</sub>:Eu) to 556 nm (CaGa<sub>2</sub>S<sub>4</sub>:Eu).<sup>12</sup> They all can meet the application requirements for GaN based LEDs.

The ZnGa<sub>2</sub>S<sub>4</sub> compounds have a bandgap at 3.18 eV and are expected as excellent phosphors.<sup>13</sup> It has a defect chalcopyrite structure by replacing a half of Zn site cations with vacancies and belongs to the *I42m* tetragonal structure.<sup>14,15</sup> Each metal atom is tetrahedrally surrounded by four sulfur atoms, while a sulfur atom is tetrahedrally surrounded by one Zn atom, two Ga atoms, and one vacancy.<sup>16</sup> The photoluminescence properties of ZnGa<sub>2</sub>S<sub>4</sub>:Eu<sup>2+</sup> have been investigated several years ago.<sup>17–20</sup> The excitation spectrum of ZnGa<sub>2</sub>S<sub>4</sub>:Eu<sup>2+</sup> indicated that ZnGa<sub>2</sub>S<sub>4</sub>:Eu<sup>2+</sup> phosphor can be used in light-emitting diode. However, its diffuse reflectance spectra, photoluminescence decay, thermal quenching, and chromaticity coordinates properties as a phosphor for LEDs have been never reported yet. In this work, we synthesized Eu<sup>2+</sup>-doped ZnGa<sub>2</sub>S<sub>4</sub> thiogallate phosphors by high temperature solid-state reactions, and described some new luminescent properties of the phosphors.

### Experimental

Ga<sub>2</sub>S<sub>3</sub> was prepared from Ga<sub>2</sub>O<sub>3</sub> (A.R.) under flowing H<sub>2</sub>S gas at 950°C for 2 h. EuS was prepared from Eu<sub>2</sub>O<sub>3</sub> (99.99%) with CS<sub>2</sub> reducing atmosphere at 1200°C for 3 h. Stoichiometric amount of raw materials, ZnO (A.R.), Ga<sub>2</sub>S<sub>3</sub> (self-prepared), and EuS (self-prepared) were mixed homogeneously and sintered for 2 h at 950°C in a flowing H<sub>2</sub>S stream. In the initial and the final heat-treatment stages, the H<sub>2</sub>S

was replaced by Ar to prevent the possible oxidation of the mixture at temperatures below 700°C.

The structure of the final products was determined via X-ray powder diffraction (XRD) using a Rigaku D/max 2200 vpc X-ray diffractometer with Cu K $\alpha$  radiation at 40 kV and 30 mA. The XRD patterns were obtained in the 15° ≤ 2 $\theta$  ≤ 70° range. The photoluminescence (PL) and photoluminescence excitation (PLE) spectra of ZnGa<sub>2</sub>S<sub>4</sub>:Eu<sup>2+</sup> were measured using a Fluorolog-3 spectrofluorometer (Jobin Yvon Inc/specx) equipped with a 450 W Xe lamp and double excitation monochromators. The decay curves and temperature-dependent PL spectra of the phosphor ZnGa<sub>2</sub>S<sub>4</sub>:Eu<sup>2+</sup> were recorded by a FLS920-Combined Fluorescence Lifetime and Steady State Spectrometer (Edinburgh Instruments), equipped with a 450 W xenon lamp, a 150 W nF900 nanosecond flash lamp with a pulse width of 1 ns and pulse repetition rate of 40–100 kHz.

### Results and Discussion

*Phase characterization.*— The crystal structure of ZnGa<sub>2</sub>S<sub>4</sub> has been refined to be tetragonal, space group *I42m* with *a* = 5.297 Å, *c* = 10.363 Å, and *V* = 290.77 Å<sup>3</sup>.<sup>15</sup> The as-prepared ZnGa<sub>2</sub>S<sub>4</sub>:0.01Eu<sup>2+</sup> sample was characterized by X-ray diffraction (XRD) patterns to verify the phase purity. As indicated in Fig. 1, we have observed that the doped Eu<sup>2+</sup> ions have no obvious influence on the structure of the host, and all the diffraction peaks of the ZnGa<sub>2</sub>S<sub>4</sub>:0.01Eu<sup>2+</sup> sample were in good agreement with the phase of ZnGa<sub>2</sub>S<sub>4</sub> (JCPDS

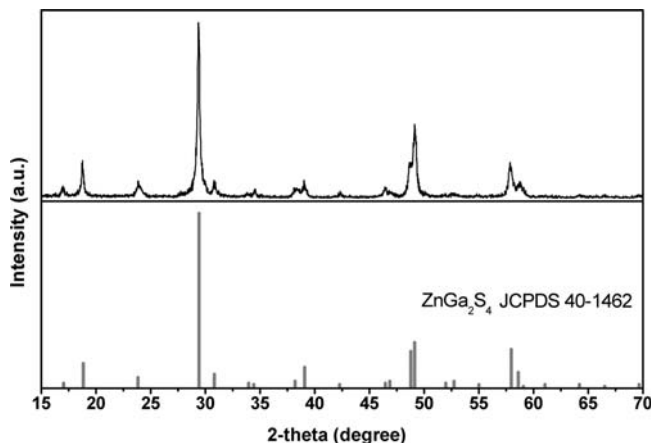
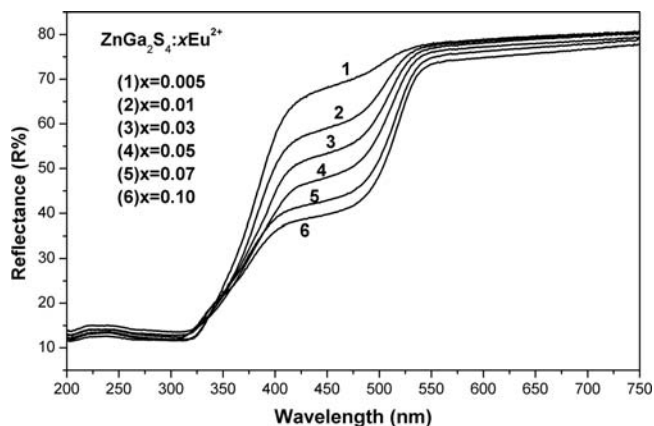


Figure 1. XRD pattern of ZnGa<sub>2</sub>S<sub>4</sub>:0.01Eu<sup>2+</sup> phosphor.

\* Electrochemical Society Active Member.

<sup>z</sup> E-mail: jhjeong@pknu.ac.kr



**Figure 2.** Diffuse reflectance spectra of  $\text{ZnGa}_2\text{S}_4:\text{xEu}^{2+}$  with different  $\text{Eu}^{2+}$  concentrations.

40-1462). The lattice parameters  $a = 5.293 \text{ \AA}$  and  $c = 10.473 \text{ \AA}$  obtained from the XRD pattern of the  $\text{ZnGa}_2\text{S}_4:0.01\text{Eu}^{2+}$  sample are in agreement with the literature data.<sup>15</sup>

The diffuse reflectance spectra of the phosphors were measured and are shown in Fig. 2. The absorption peaks of all the samples are similar in their spectral features with a little difference in the relative intensity with  $\text{Eu}^{2+}$  concentration increases. It can be seen that the strong absorptions in the range 250–350 nm do not almost change with the increase of  $\text{Eu}^{2+}$  concentration, which is attributed to the absorption of the host. Another strong absorption occurs from the UV to the visible spectral region (370–550 nm), which is caused by the  $4f^7 \rightarrow 4f^6 5d^1$  transition of the  $\text{Eu}^{2+}$  ion. With the  $\text{Eu}^{2+}$  concentration increasing, this absorption becomes stronger, which yields the phosphor powder color varying from pale green to dark green.

The PL excitation and emission spectra of  $\text{ZnGa}_2\text{S}_4:0.05\text{Eu}^{2+}$  are shown in Fig. 3. The excitation spectrum exhibits a broad absorption from 350 to 520 nm, which are attributed to the host absorption and the  $4f^7(^8\text{S}_{7/2}) \rightarrow 4f^6(^7\text{F})5d^1$  transitions of  $\text{Eu}^{2+}$  ion, and consistent with the diffuse reflectance spectra as presented in Fig. 3. Because the broad excitation matches well with Ga(In)N chip emission,  $\text{ZnGa}_2\text{S}_4:\text{xEu}^{2+}$  phosphors are suitable for n-UV or blue LED chip excited solid state lighting. As it has a broad excitation, this phosphor can be excited with different wavelengths. It can be seen from Figs. 3b and 3c,  $\text{ZnGa}_2\text{S}_4:0.05\text{Eu}^{2+}$  phosphor shows a green emission band peaking at 540 nm under 395- and 460-nm excitations. No differences are observed for the emission band shape and position for different excitation wavelengths except for the luminescent intensity. The full width at half maximum (fwhm) of the emission spectrum (curve c) is 47 nm. These results coincide well with those of Yuta and Whit<sup>17</sup> while the maximum (565 nm) as well as the fwhm (about 100 nm) presented by Tagiev et al.<sup>18</sup> show no agreement.

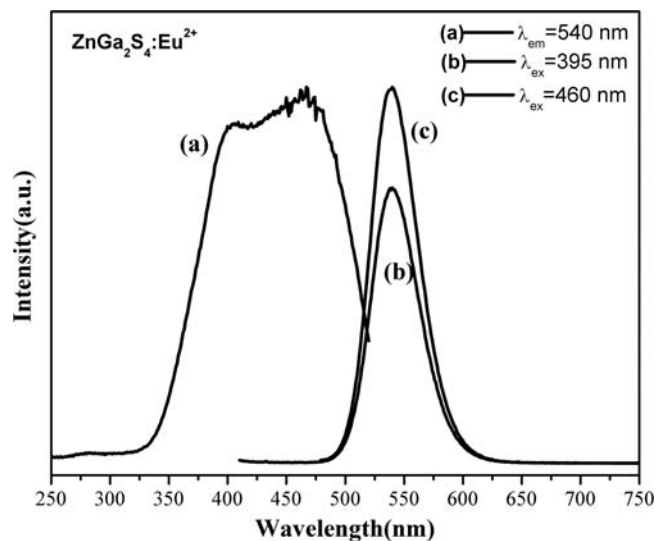


**Figure 3.** Excitation (a,  $\lambda_{\text{em}} = 540 \text{ nm}$ ) and emission (b,  $\lambda_{\text{ex}} = 395 \text{ nm}$ ; c,  $\lambda_{\text{ex}} = 460 \text{ nm}$ ) spectra of  $\text{ZnGa}_2\text{S}_4:\text{Eu}^{2+}$ .

The CIE chromaticity coordinates of  $\text{ZnGa}_2\text{S}_4:0.05\text{Eu}^{2+}$  phosphor are calculated in terms of the emission spectrum, and the value are  $x = 0.299$ ,  $y = 0.673$ . Since the excitation spectra are not well resolved, the position of the lowest 5d excited level of  $\text{Eu}^{2+}$  ( $\lambda_{\text{abs}}$ ) is generally estimated by using the mirror-image relationship between the emission and the excitation spectra.<sup>21,22</sup> The Stokes shift ( $\Delta S$ ) can be estimated by taking twice the energy difference between the zero phonon line and the energy of the emission maximum. The position of the zero phonon line is taken to be the intersection point of the excitation and emission spectra.<sup>23</sup> In the present case, the lowest absorption energy of  $E_{\text{abs}}$  is about 2.52 eV (492 nm) and the Stokes shift ( $\Delta S$ ) is calculated to be 0.22 eV ( $1772 \text{ cm}^{-1}$ ).

Recently the PL properties of  $\text{Eu}^{2+}$ -activated  $\text{MGa}_2\text{S}_4$  ( $M = \text{Ca}, \text{Sr}, \text{Ba}$ ) thiogallate compounds for LEDs have been studied.<sup>7-10,24</sup> The crystallographic data of  $\text{MGa}_2\text{S}_4$  and the luminescence characteristics of  $\text{MGa}_2\text{S}_4:\text{Eu}^{2+}$  are summarized in Table I. Usually  $\text{Eu}^{2+}$  ions exhibit broad-band emission, which is attributed to the  $4f^6 5d^1 - 4f^7$  transition, and the wavelength positions of the emission bands depend very much on a host, changing from the n-UV to the red. Although these compounds have similar chemical compositions, their crystal structures are different. Previous works reported that the emission wavelengths of  $\text{MGa}_2\text{S}_4:\text{Eu}^{2+}$  shifted to longer wavelengths (red-shift) as replacing M atoms with smaller ones due to larger crystal field splitting. Such as  $\text{BaGa}_2\text{S}_4:\text{Eu}^{2+}$  ( $\lambda_{\text{em}} = 504 \text{ nm}$ ),  $\text{SrGa}_2\text{S}_4:\text{Eu}^{2+}$  ( $\lambda_{\text{em}} = 535 \text{ nm}$ ), and  $\text{CaGa}_2\text{S}_4:\text{Eu}^{2+}$  ( $\lambda_{\text{em}} = 558 \text{ nm}$ ). The red-shift and the emission wavelengths generally increase with decreasing the size of 'M' cation ( $\text{Ba}^{2+} = 1.36 \text{ \AA}$ ,  $\text{Sr}^{2+} = 1.26 \text{ \AA}$ ,  $\text{Ca}^{2+} = 1.12 \text{ \AA}$ ).

**Table I.** Crystallographic data of  $\text{MGa}_2\text{S}_4$  and the luminescence characteristics of  $\text{MGa}_2\text{S}_4:\text{Eu}^{2+}$  ( $M = \text{Ca}, \text{Sr}, \text{Ba}, \text{Zn}$ ).

Formula	$\text{CaGa}_2\text{S}_4$	$\text{SrGa}_2\text{S}_4$	$\text{BaGa}_2\text{S}_4$	$\text{ZnGa}_2\text{S}_4$
Crystal system	Orthorhombic	Orthorhombic	Cubic	Tetragonal
Space group	$D_{2h}^{24}\text{-Fddd}$	$D_{2h}^{24}\text{-Fddd}$	$\text{Th}^6\text{-Pa}3$	$I4_2m$
a (Å)	20.122	20.855	12.685	5.293
b (Å)	20.090	20.511	12.685	5.293
c (Å)	12.133	12.213	12.685	10.473
V (Å <sup>3</sup> )	4904	5224	2041	293
Emission (nm)	558	535	504	540
fwhm (nm)	50	49	62	47
Stokes shift (cm <sup>-1</sup> )	2079	2000	4000	1772
CIE	(0.410, 0.580)	(0.270, 0.690)	(0.143, 0.506)	(0.299, 0.673)
References	5,9,12	5,9,12	5,21	This work, <sup>15</sup>

Theoretically,  $\text{ZnGa}_2\text{S}_4:\text{Eu}^{2+}$  had to show the longer wavelength emission than  $\text{SrGa}_2\text{S}_4:\text{Eu}^{2+}$  and  $\text{CaGa}_2\text{S}_4:\text{Eu}^{2+}$  because Zn atomic size was much smaller than Sr and Ca. However, in this experiment, the emission wavelength of  $\text{ZnGa}_2\text{S}_4:\text{Eu}^{2+}$  was almost same with that of  $\text{SrGa}_2\text{S}_4:\text{Eu}^{2+}$ . Even though  $\text{Zn}^{2+}$  size was smaller than  $\text{Sr}^{2+}$ , the lattice parameter of  $\text{ZnGa}_2\text{S}_4$  was also small comparing with  $\text{SrGa}_2\text{S}_4$ , leading to the almost same crystal field splitting energy, and so emission bands of these two phosphors were located at the similar wavelength. Therefore, the red-shift did not apply to  $\text{ZnGa}_2\text{S}_4:\text{Eu}^{2+}$  in spite of the even smaller ionic radius of  $\text{Zn}^{2+}$ .<sup>25</sup>

It is generally accepted that the  $\text{Eu}^{2+}$  concentration plays an important role in the searching of optimal composition of phosphor. Therefore, the emission spectra of  $\text{ZnGa}_2\text{S}_4:\text{Eu}^{2+}$  at various concentrations excited by 460 nm light and the dependence of PL intensity of  $\text{Zn}_{1-x}\text{Ga}_2\text{S}_4:x\text{Eu}^{2+}$  on  $\text{Eu}^{2+}$  concentration ( $x = 0.005\text{--}0.10$ ) are shown in Fig. 4. It is observed that the PL intensity increases with the increasing of  $\text{Eu}^{2+}$  content until reaches a maximum at  $x = 0.05$ , then it falls steadily as the content of  $\text{Eu}^{2+}$  further increases due to concentration quenching, which is mainly caused by the non-radiative energy transfer among the identical  $\text{Eu}^{2+}$  ions. The quench concentration is very close to the reported value  $x = 0.04$ .<sup>20</sup>

While discussing the mechanism of energy transfer in phosphors, Blasse has pointed out that if the activator is introduced solely on Z ion sites,  $x_c$  is the critical concentration, N the number of Z ions in the unit cell and V the volume of the unit cell, then there is on the average one activator ion per  $V/x_c N$ .<sup>26</sup> From Fig. 4, it is clear that 0.05 mol is the critical concentration of  $\text{Eu}^{2+}$ . The critical transfer distance ( $R_c$ ) is approximately equal to twice the radius of a sphere with this volume:

$$R_c \approx 2 \left( \frac{3V}{4\pi x_c N} \right)^{1/3} \quad [1]$$

By taking the appropriate values of V, N and  $x_c$  ( $298.27 \text{ \AA}^3$ , 2, and 0.05, respectively), the critical transfer distance of center  $\text{Eu}^{2+}$  in  $\text{ZnGa}_2\text{S}_4:\text{Eu}^{2+}$  phosphor was found to be  $17 \text{ \AA}$ . Non-radiative energy transfer between different  $\text{Eu}^{2+}$  ions may occur by exchange interaction, radiation reabsorption, or multipole-multipole interaction.<sup>27,28</sup>  $\text{Eu}^{2+}$  is an isolated emission center in  $\text{ZnGa}_2\text{S}_4:\text{Eu}^{2+}$  phosphor. The  $4f^6 5d^1\text{--}4f^7$  transition of  $\text{Eu}^{2+}$  is allowed while exchange interaction is responsible for the energy transfer for forbidden transitions and typical critical distances are then about  $5^\circ \text{A}$ .<sup>29</sup> This indicates that the mechanism of exchange interaction plays no role in energy transfer between  $\text{Eu}^{2+}$  ions in  $\text{ZnGa}_2\text{S}_4:\text{Eu}^{2+}$  phosphor. The mechanism of

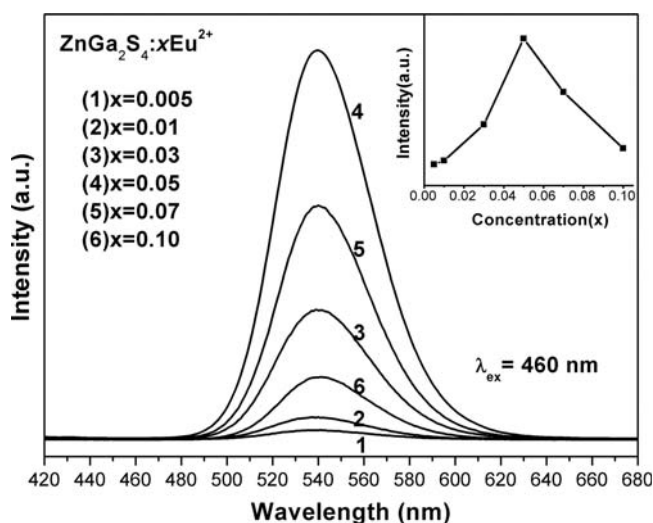


**Figure 4.** Dependence of PL intensities of  $\text{ZnGa}_2\text{S}_4:x\text{Eu}^{2+}$  ( $\lambda_{\text{ex}} = 460 \text{ nm}$ ) with varying  $\text{Eu}^{2+}$  concentrations. The upper inset represents the concentration influence on the emission intensities of  $\text{ZnGa}_2\text{S}_4:x\text{Eu}^{2+}$  phosphors ( $x = 0.005, 0.01, 0.03, 0.05, 0.07, \text{ and } 0.10$ ).

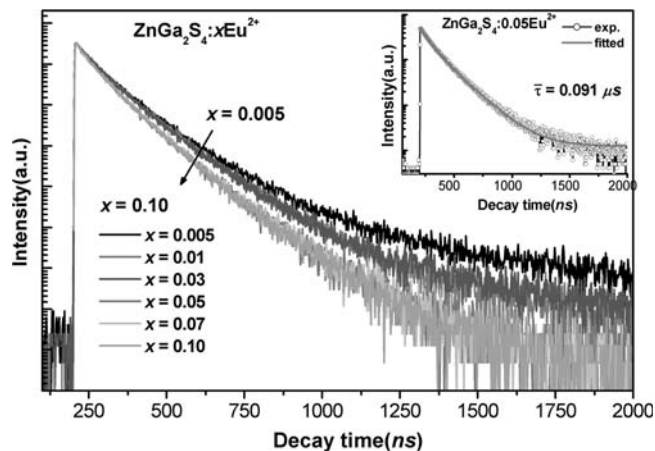


**Figure 5.** The decay curves of  $\text{Eu}^{2+}$  in  $\text{ZnGa}_2\text{S}_4:x\text{Eu}^{2+}$  at different concentrations ( $\lambda_{\text{ex}} = 460 \text{ nm}$ ,  $\lambda_{\text{em}} = 540 \text{ nm}$ ) ( $x = 0.005, 0.01, 0.03, 0.05, 0.07, \text{ and } 0.10$ ).

radiation re-absorption comes into effect only when there is broad overlap of the fluorescent spectra of the sensitizer and activator and in the view of the emission and excitation spectra of  $\text{ZnGa}_2\text{S}_4:\text{Eu}^{2+}$  phosphor is unlikely to be occurring in the case. Since the fluorescent mechanism of  $\text{Eu}^{2+}$  in  $\text{ZnGa}_2\text{S}_4:\text{Eu}^{2+}$  phosphor is the  $4f\text{--}5d$  allowed electric-dipole transition, the process of energy transfer should be controlled by electric multipole-multipole interaction according to Dexter's theory.<sup>29,30</sup>

The decay curves of  $\text{Eu}^{2+}$  in the phosphor  $\text{ZnGa}_2\text{S}_4:x\text{Eu}^{2+}$  have been measured at different concentrations ( $x = 0.005, 0.01, 0.03, 0.05, 0.07, \text{ and } 0.10$ ) ( $\lambda_{\text{ex}} = 460 \text{ nm}$ ,  $\lambda_{\text{em}} = 540 \text{ nm}$ ). The emission decay curves of  $\text{Eu}^{2+}$  ion are well fitted with a second order exponential Equation 2<sup>31</sup>:

$$I(t) = A_1 \exp(-t/\tau_1) + A_2 \exp(-t/\tau_2) \quad [2]$$

where  $I$  is the luminescence intensity,  $t$  is time,  $\tau_1$  and  $\tau_2$  are the slow and fast components of the decay lifetimes, and  $A_1$  and  $A_2$  are the fitting parameters, respectively. The average lifetimes of  $\text{Eu}^{2+}$ ,  $\bar{\tau}$ , could be calculated as Equation 3<sup>32</sup>:

$$\bar{\tau} = \frac{A_1 \tau_1^2 + A_2 \tau_2^2}{A_1 \tau_1 + A_2 \tau_2} \quad [3]$$

A representative pattern is shown in the inset of Fig. 5. The average lifetimes of  $\text{Eu}^{2+}$  ions were determined to be 0.126, 0.115, 0.102, 0.091, 0.085 and 0.079  $\mu\text{s}$  for  $\text{ZnGa}_2\text{S}_4:x\text{Eu}^{2+}$  with  $x = 0.005, 0.01, 0.03, 0.05, 0.07$  and  $0.10$ , respectively (Table II). With the concentration increasing, the lifetime values decrease, due to the parity allowed electric dipole transitions of  $\text{Eu}^{2+}$  ions with high transition probabilities. The decay times of these transitions are submicroseconds. Generally, at high concentrations of  $\text{Eu}^{2+}$ , the migration of energy nonradiatively between the  $\text{Eu}^{2+}$  increases, resulting in a decrease in the lifetime.

In the solid-state lighting application, a lower-temperature quenching effect is in favor of keeping the chromaticity and brightness of white light output. The temperature dependence of the PL spectra for the  $\text{ZnGa}_2\text{S}_4:0.05\text{Eu}^{2+}$  phosphor under excitation at 460 nm is shown in Fig. 6. With an increase in temperature from 300 K to 480 K, the PL intensity decreases slowly. The thermal quenching

**Table II.** The lifetimes of  $\text{Eu}^{2+}$  in  $\text{ZnGa}_2\text{S}_4:x\text{Eu}^{2+}$  at different concentrations ( $\lambda_{\text{ex}} = 460 \text{ nm}$ ,  $\lambda_{\text{em}} = 540 \text{ nm}$ ) ( $x = 0.005, 0.01, 0.03, 0.05, 0.07, \text{ and } 0.10$ ).

Concentration	0.005	0.01	0.03	0.05	0.07	0.10
$\bar{\tau}$ ( $\mu\text{s}$ )	0.126	0.115	0.102	0.091	0.085	0.079

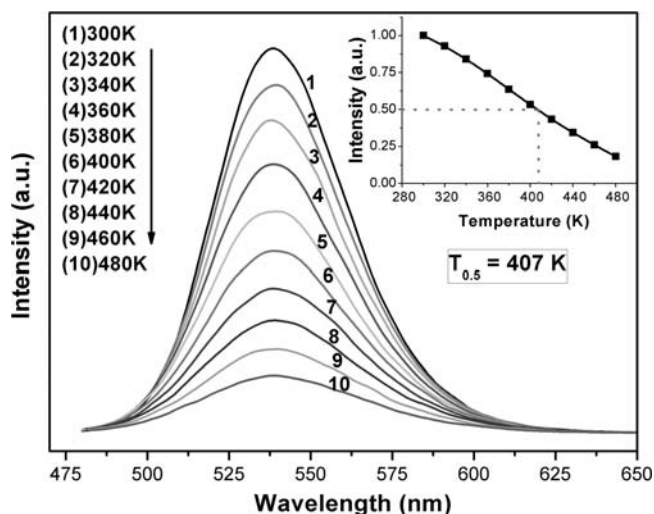


**Figure 6.** Dependence of PL emission of  $\text{ZnGa}_2\text{S}_4:0.05\text{Eu}^{2+}$  ( $\lambda_{\text{ex}} = 460$  nm) on temperature. The inset shows the relationship of relative intensity and temperature.

temperature  $T_{50}$  defined as the temperature at which the emission intensity is 50% of its original value, is 407 K for  $\text{ZnGa}_2\text{S}_4:0.05\text{Eu}^{2+}$ . With heating the sample up to 420 K at which the LEDs usually work, the emission intensity of it remains at about 44% of that measured at room temperature. Dorenbos has proposed that the main mechanism responsible for the thermal quenching of  $5d-4f$  emission of  $\text{Eu}^{2+}$  in solids is the ionization of the electron from the lowest energy level of the relaxed  $\text{Eu}^{2+} 4f^6 5d^1$  electronic configuration to the host lattice conduction band level.<sup>30,33</sup> Following this suggestion, it is responsible that the thermally activated ionization from the excited  $5d$  state of the  $\text{Eu}^{2+}$  ion is for temperature quenching of the luminescence in  $\text{ZnGa}_2\text{S}_4:\text{Eu}^{2+}$ . The temperature dependence of the luminescence intensity is described by the following Arrhenius equation<sup>34,35</sup>

$$I(T) = \frac{I_0}{1 + c \exp(-E/kT)} \quad [4]$$

where  $I_0$  is the initial intensity,  $I(T)$  is the intensity at a given temperature  $T$ ,  $c$  is a constant,  $E$  is the activation energy, which represents the energy difference between the lowest excited state and the bottom of the host lattice conduction band, and  $k$  is Boltzmann's constant ( $8.62 \times 10^{-5}$  eV). Figure 7 plots  $\ln[(I_0/I)-1]$  vs.  $1/T$ . When performing lin-

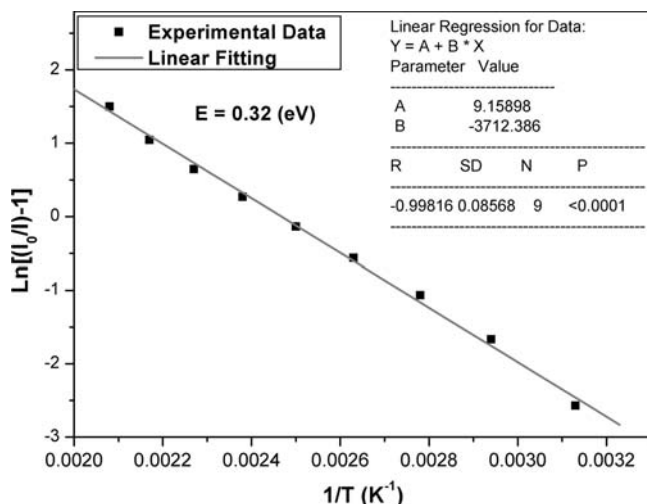


**Figure 7.** Arrhenius plot of the temperature dependence of the PL emission intensity of  $\text{ZnGa}_2\text{S}_4:0.05\text{Eu}^{2+}$ .

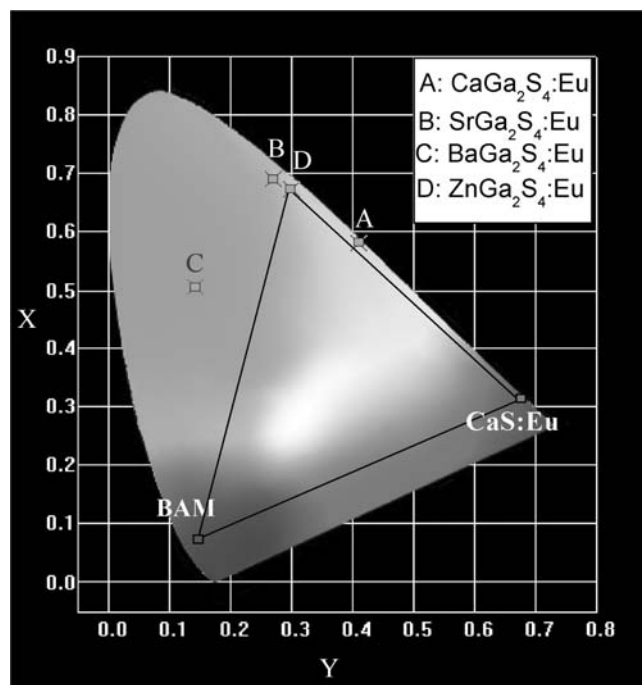


**Figure 8.** The CIE chromaticity diagram of  $\text{MGa}_2\text{S}_4:\text{Eu}^{2+}$  ( $M = \text{Ca}, \text{Sr}, \text{Ba}, \text{Zn}$ ) phosphors.

ear regression, the thermal activation energy for quenching is found to be  $\sim 0.32$  eV.

The Commission International de l'Éclairage (CIE) chromaticity coordinates of the  $\text{MGa}_2\text{S}_4:\text{Eu}^{2+}$  ( $M = \text{Ca}, \text{Sr}, \text{Ba}, \text{Zn}$ ) phosphors were depicted in Fig. 8 in form of four rectangles. The chromaticity coordinates of phosphors  $\text{CaS}:\text{Eu}^{2+}$  (0.680, 0.310) and  $\text{BaMgAl}_{10}\text{O}_{17}:\text{Eu}^{2+}$  (BAM) (0.144, 0.072), which are two primary color phosphors used for fluorescent lamps, are also depicted in the figure. The chromaticity coordinates of  $\text{ZnGa}_2\text{S}_4:\text{Eu}^{2+}$  phosphor fall into the green region and are very close to those of  $\text{SrGa}_2\text{S}_4:\text{Eu}^{2+}$ . It is due to the similarity of the photoluminescence spectra of both phosphors. As we can see, if combined with other high efficiency blue and red phosphors,  $\text{ZnGa}_2\text{S}_4:\text{Eu}^{2+}$  should be a good green component phosphor for UV-excited white LEDs.

## Conclusions

Here, a green  $\text{Eu}^{2+}$ -activated  $\text{ZnGa}_2\text{S}_4$  thiogallate phosphor has been synthesized by solid-state reaction and its luminescent properties are investigated. The excitation and emission spectra of this phosphor show that all are broadband due to  $4f^7-4f^6 5d^1$  transitions of  $\text{Eu}^{2+}$ . The PL emission spectrum shows a broad band peaking at 540 nm. The luminescence characteristics of thiogallate phosphors  $\text{MGa}_2\text{S}_4:\text{Eu}^{2+}$  ( $M = \text{Ca}, \text{Sr}, \text{Ba}, \text{Zn}$ ) have been compared in this paper. The optimal concentration for  $\text{Eu}^{2+}$  in  $\text{ZnGa}_2\text{S}_4$  is about 5 mol%. The critical transfer distance of  $\text{Eu}^{2+}$  is calculated as 17 Å and the mechanism of concentration quenching is determined to be the multipole-multipole interaction. The thermal quenching result suggests that the phosphor does not have good thermal-quenching property. The energy barrier for thermal quenching is confirmed as 0.32 eV by the Arrhenius equation. Its chromaticity coordinates are very close to those of  $\text{SrGa}_2\text{S}_4:\text{Eu}$ . Because of their broadband absorption in the region 350–520 nm, the  $\text{ZnGa}_2\text{S}_4:0.05\text{Eu}^{2+}$  phosphor can be a good green phosphor candidate for creating white light in phosphor-converted white LEDs, when combined with RB phosphors and a UV LED.

### Acknowledgments

This work was supported by Chinese Universities Scientific Fund (QN2011119). And this research was supported by the Industrials Strategic Technology Development Program (Project No: 10037416) funded by the Ministry of Knowledge Economy (MKE, Korea).

### References

1. T. E. Peters and J. A. Baglio, *J. Electrochem. Soc.*, **119**, 230 (1972).
2. T. E. Peters, *J. Electrochem. Soc.*, **119**, 1720 (1972).
3. M. Y. Kim, S. J. Baik, W. T. Kim, M. S. Jin, H. G. Kim, S. H. Choe, and C. S. Yoon, *J. Korean Phys. Soc.*, **43**, 128 (2003).
4. C. Guo, Q. Tang, D. Huang, C. Zhang, and Q. Su, *Mater. Res. Bull.*, **42**, 2032 (2007).
5. M. Nazarov, D. Y. Noh, and H. Kim, *Mater. Chem. Phys.*, **107**, 456 (2008).
6. H. J. Yu, W. Chung, S. H. Park, J. Kim, and S. H. Kim, *Mater. Lett.*, **65**, 474 (2010).
7. J. M. Kim, K. N. Kim, S. H. Park, J. K. Park, C. H. Kim, and H. G. Jang, *J. Korean Chem. Soc.*, **49**, 201 (2005).
8. J. M. Kim, J. K. Park, K. N. Kim, S. J. Lee, C. H. Kim, and H. G. Jang, *J. Korean Chem. Soc.*, **50**, 237 (2006).
9. Y. R. Do, K.-Y. Ko, S.-H. Na, and Y.-D. Huh, *J. Electrochem. Soc.*, **153**, H142 (2006).
10. X. Zhang, W. Hao, H. Zeng, and S. Qiang, *J. Rare Earths*, **25**, 701 (2007).
11. M. Nagata, S. Okamoto, K. Tanaka, T. Sakai, H. Kawasaki, and A. Tamaki, *J. Lumin.*, **130**, 2040 (2010).
12. R. Yu, J. Wang, M. Zhang, H. Yuan, W. Ding, Y. An, and Q. Su, *J. Electrochem. Soc.*, **155**, J290 (2008).
13. H. G. Kim and W. T. Kim, *Phys. Rev. B: Condens. Matter*, **41**, 8541 (1990).
14. G. B. Carpenter, P. Wu, Y. M. Gao, and A. Wold, *Mater. Res. Bull.*, **24**, 1077 (1989).
15. J. Zhang, W. W. Chen, A. J. Ardell, and B. Dunn, *J. Am. Ceram. Soc.*, **73**, 1544 (1990).
16. A. Eifler, G. Krauss, V. Riede, V. Kraemer, and W. Grill, *J. Phys. Chem. Solids*, **66**, 2052 (2005).
17. M. M. Yuta and W. B. White, *J. Electrochem. Soc.*, **139**, 2347 (1992).
18. B. G. Tagiev, G. G. Guseinov, R. B. Dzhabbarov, O. B. Tagiev, N. N. Musaeva, and A. N. Georgobiani, *Inorg. Mater.*, **36**, 1189 (2000).
19. C. Wickleder, S. Zhang, and H. Haeuseler, *Z. Kristallogr.*, **220**, 277 (2005).
20. J. W. Kim and Y. J. Kim, *J. Eur. Ceram. Soc.*, **27**, 3667 (2007).
21. R. B. Jabbarov, C. Chartier, B. G. Tagiev, O. B. Tagiev, N. N. Musayeva, C. Barthou, and P. Benalloul, *J. Phys. Chem. Solids*, **66**, 1049 (2005).
22. C. Barthou, R. B. Jabbarov, P. Benalloul, C. Chartier, N. N. Musayeva, B. G. Tagiev, and O. B. Tagiev, *J. Electrochem. Soc.*, **153**, G253 (2006).
23. V. Bachmann, T. Jüstel, A. Meijerink, C. Ronda, and P. J. Schmidt, *J. Lumin.*, **121**, 441 (2006).
24. R. Yu, J. Wang, J. Zhang, and Q. Su, *J. Electrochem. Soc.*, **158**, J86 (2011).
25. P. Dorenbos, *J. Lumin.*, **104**, 239 (2003).
26. L. G. Van Uitert, *J. Electrochem. Soc.*, **114**, 1048 (1967).
27. G. Blasse and B. C. Grabmaier, *Luminescent Materials*, p. 46, Springer-Verlag, Berlin, Heidelberg (1994).
28. D. L. Dexter, *J. Chem. Phys.*, **21**, 836 (1953).
29. G. Blasse, *Phys. Lett. A*, **28**, 444 (1968).
30. P. Dorenbos, *J. Phys.: Condens. Matter*, **17**, 8103 (2005).
31. R. K. Bauer, R. Borenstein, P. De Mayo, K. Okada, M. Rafalska, W. R. Ware, and K. C. Wu, *JACS*, **104**, 4635 (1982).
32. T. Fujii, K. Kodaira, O. Kawauchi, N. Tanaka, H. Yamashita, and M. Anpo, *J. Phys. Chem. B*, **101**, 10631 (1997).
33. R. J. Yu, B. Deng, G. G. Zhang, Y. An, J. H. Zhang, and J. Wang, *J. Electrochem. Soc.*, **158**, J255 (2011).
34. S. Bhushan and M. V. Chukichev, *J. Mater. Sci. Lett.*, **7**, 319 (1988).
35. V. Bachmann, C. Ronda, O. Oeckler, W. Schnick, and A. Meijerink, *Chem. Mater.*, **1**, 316 (2009).